10$^{\text{th}}$ World Congress on Structural and Multidisciplinary Optimization
May 19 - 24, 2013, Orlando, Florida, USA

Distributed loads in truss topology optimization

Kristo Mela and Juhani Koski

Tampere University of Technology – Department of Engineering Design
P.O.Box 589, FI-33101 Tampere, Finland
e-mail: kristo.mela@tut.fi

1. Abstract
In this work, a method for incorporating distributed loads in truss topology optimization is presented. The ground structure is supplemented with overlapping members between each pair of nodes subject to the distributed load, and binary variables controlling the existence of the members and nodes are introduced. Equivalent nodal loads are computed for all members under the line load. The binary variables are used to switch off the equivalent nodal loads of vanishing members from the equilibrium equations. Linear constraints in the binary variables disallow overlapping members from the optimum solution.
The proposed method is employed in a linear mixed-integer formulation of minimum weight truss topology optimization problem. The effects of the methods are demonstrated on a roof truss design problem. The example problem illustrates the important feature of the method that allows grouns structure nodes under line loads to vanish.
2. Keywords: Truss topology optimization, distributed loads, mixed variable formulation.

3. Introduction
Structures are often subject to distributed loads such as wind, snow, and inertial forces. In skeletal structures, the distributed loads act along the members that are defined as lines in the structural model. In truss analysis, distributed loads are transformed into equivalent nodal loads, and the effects of bending are neglected.
In the literature on truss topology optimization, distributed loads are seldom treated. In fact, often only point loads resembling a distributed load are considered, as in the bridge examples in [10, 1]. In [9], the distributed load is discretized according to the ground structure such that equivalent nodal (point) loads are computed for the nodes of the ground structure under the distributed load. However, as all loaded nodes of the ground structure must be present in the optimum solution, this approach does not allow nodes under the distributed load to vanish, even if it would lead to better design. Also, if the ground structure is made denser, the number of loaded nodes increases, which generally leads to an increase in the number of members in the optimum truss.
In this paper, a formulation for incorporating distributed loads into truss topology optimization is proposed. The ground structure approach [4] is employed. The method is based on binary variables that control the existence of ground structure members and nodes. Overlapping members are added between all nodes subject to the distributed load. Equivalent nodal loads for all of these members are included in the equilibrium equations, and the binary variables are used to switch off the nodal loads of vanishing members. Further constraints ensure sufficient support for the loaded nodes and disallow member overlapping in the optimum structure.
The binary variables controlling member existence fit well into the mixed-integer formulation proposed for truss topology optimization [6, 12]. In this formulation, member forces and nodal displacements are taken as continuous state variables and binary variables are employed to control member and node existence as well as to choose member cross-sections. Essentially, the present work extends the earlier mixed-integer formulations such that distributed loads are including in the problem properly.
The paper is organized as follows. First, the mixed-integer formulation is briefly revised. Then, in Section 5, the proposed approach for distributed loads is presented. The method is illustrated on a test problem of topology optimization of a roof truss in Section 6. The paper ends with discussion and conclusions.

4. Mixed Variable Formulation of Minimum Weight Problem
Commonly, the minimum weight problem for trusses is formulated using the *nested analysis and design* (NAND) approach, where the cross-sectional areas of the ground structure members are the design vari-

ables, and structural responses, such as stresses, are evaluated by the finite element method. Another approach is to write the equations of structural analysis as equality constraints and take nodal displacements and member forces as optimization variables. For topology optimization, this *simultaneous analysis and design* (SAND) approach [2] is fruitful, since by disaggregating the stiffness equation to element level, the singularities related to vanishing members can be avoided. Also, for discrete cross-sections, this approach leads to a *mixed-integer linear optimization* (MILP) problem, for which powerful solution software is available. In the present work, the MILP formulation presented in [12] is adopted and extended from other sources of literature.

4.1. Basic Formulation

Suppose the member cross-sections are to be chosen from a discrete set of n_S alternatives. The cross-sectional area of alternative j is denoted $\hat{A}_j$. Denote the index set of members of the ground structure $\mathcal{M} = \{1, 2, \ldots, n_E\}$. The set of ground structure nodes is $\mathcal{N} = \{1, 2, \ldots, n_N\}$. The set of loading conditions is $\mathcal{L} = \{1, 2, \ldots, n_L\}$, and the set of available profiles is $\mathcal{P} = \{1, 2, \ldots, n_S\}$.

Member cross-section is selected by the binary variable y_{ij}, which takes the value 1, if profile j is chosen for member i and 0 otherwise. Binary variables y_i, $i \in \mathcal{M}$ control member existence: $y_i = 1$ if member i is present and $y_i = 0$ otherwise. Finally, binary variables z_ℓ, $\ell \in \mathcal{N}$ control the existence of nodes: if $z_\ell = 1$, then node ℓ is present in the truss and $z_\ell = 0$ otherwise.

The continuous variables are member normal forces, N_{ij}^k and nodal displacements $\mathbf{u}^k$, $i \in \mathcal{M}$, $j \in \mathcal{P}$, $k \in \mathcal{L}$. The variable N_{ij}^k is the normal force of member i in load case k for profile j and $\mathbf{u}^k$ is the vector of nodal displacements in load case k.

With these variables, the minimum weight problem with member strength constraints can be written as

$$
\begin{aligned}
\min \quad & \sum_{i=1}^{n_E}\sum_{j=1}^{n_S} \rho L_i \hat{A}_j y_{ij} \\
\text{such that} \quad & y_i = \sum_{j=1}^{n_S} y_{ij} \quad \forall\, i \in \mathcal{M} \\
& y_i \le z_\ell \quad \forall\, \ell \in \mathcal{N},\, i \in \mathcal{M}_\ell \\
& \underline{\mathbf{u}}_\ell z_\ell \le \mathbf{u}_\ell^k \le \overline{\mathbf{u}}_\ell z_\ell \quad \forall\, \ell \in \mathcal{N},\, k \in \mathcal{L} \\
& \frac{E_i}{L_i}\hat{A}_j \mathbf{b}_i^{\mathrm{T}} \mathbf{u}^k - N_{ij}^k \le (1 - y_{ij})\overline{N}_{ij}^k \quad \forall\, i \in \mathcal{M},\, j \in \mathcal{P},\, k \in \mathcal{L} \\
& \frac{E_i}{L_i}\hat{A}_j \mathbf{b}_i^{\mathrm{T}} \mathbf{u}^k - N_{ij}^k \ge (1 - y_{ij})\underline{N}_{ij}^k \quad \forall\, i \in \mathcal{M},\, j \in \mathcal{P},\, k \in \mathcal{L} \\
& \hat{\mathbf{B}}\hat{\mathbf{N}}^k = \mathbf{p}^k \quad \forall\, k \in \mathcal{L} \\
& N_{ij}^k \le \min\{\overline{N}_{ij}^k, \overline{\sigma}\hat{A}_j\} y_{ij} \quad \forall\, i \in \mathcal{M},\, j \in \mathcal{P},\, k \in \mathcal{L} \\
& N_{ij}^k \ge \max\{\underline{N}_{ij}^k, -\underline{\sigma}\hat{A}_j\} y_{ij} \quad \forall\, i \in \mathcal{M},\, j \in \mathcal{P},\, k \in \mathcal{L} \\
& y_i, y_{ij}, z_\ell \in \{0, 1\}
\end{aligned} \tag{P}
$$

In the above, ρ is the density of the material (assumed same for all members), L_i, and E_i are the length and Young's modulus of member i, respectively, and $\mathbf{b}_i$ is the i^{th} column of the statics matrix of the ground structure. Furthermore, $\mathbf{u}_\ell^k$ is the vector of displacements of node ℓ in loading condition k, and $\underline{\mathbf{u}}_\ell$ and $\overline{\mathbf{u}}_\ell$ are the bounds for nodal displacements. These bounds are used to compute the bounds for the force variables, $\underline{N}_{ij}^k$ and $\overline{N}_{ij}^k$, see [12]. The global load vector of loading condition k is $\mathbf{p}^k$, and $\hat{\mathbf{B}}$ and $\hat{\mathbf{N}}^k$ are the extended statics matrix and force variable vector, respectively (again, see [12]).

The first constraint guarantees a unique profile for each members. Note that if $y_i = 0$, then by this constraint, $y_{ij} = 0$ for all $j \in \mathcal{P}$. The second constraint states that if node ℓ is removed, then all members connected to that node must also vanish. The last two inequality constraints are the member strength constraints, where $\underline{\sigma}$ and $\overline{\sigma}$ are the maximum allowable stresses in compression and in tension, respectively. For the other constraints, see [12].

4.2. Kinematic Stability

A common problem in truss topology optimization is that the optimum solution satisfies the equilibrium equations induced by the loads, but is kinematically unstable, i.e. a mechanism. In this work, problem P

is extended for ensuring kinematically stable solutions by employing a modification of the approach proposed in [5], see also [8]. The idea is to include an additional loading condition to the problem, where *all* free nodes of the ground structure are loaded by small predefined loads. The nodal variables z_ℓ are used to control the presence of these auxiliary loads in the equilibrium equations of the supplementary loading condition, and member forces in this loading condition are added to the continuous variables. Denote by $\mathcal{D}_\ell$ the global degrees of freedom of node ℓ. Then, the auxiliary loads for this node are

$$\tilde{p}_j = \tilde{p}_{j\ell} z_\ell \quad j \in \mathcal{D}_\ell \tag{1}$$

where $\tilde{p}_{j\ell} > 0$ are predefined values for the loads. Essentially, any values can be given to the $\tilde{p}_{j\ell}$, but they should be small enough such that they do not affect the optimum selection of member profiles. In order to minimize the possibility that the structure is a mechanism but is in equilibrium with respect to the auxiliary loads, the resultant force of the load components at a node should not be parallel to any of the members connected to that node, and all $\tilde{p}_{j\ell}$ are chosen to be positive.
The auxiliary loads can be gathered to a load vector. This is denoted by

$$\tilde{\mathbf{p}} = \mathbf{P}\mathbf{z} \in \mathbb{R}^{n_d} \tag{2}$$

where $\mathbf{P} \in \mathbb{R}^{n_d \times n_N}$. The elements of $\mathbf{P}$ are $P_{ij} = \tilde{p}_{ij}$, when $i \in \mathcal{D}_j$ and $P_{ij} = 0$ otherwise. The nodal equilibrium is then expressed in matrix form as

$$\mathbf{B}\tilde{\mathbf{N}} = \tilde{\mathbf{p}} = \mathbf{P}\mathbf{z} \tag{3}$$

where $\mathbf{B}$ is the statics matrix of the ground structure and $\tilde{\mathbf{N}}$ is the vector of auxiliary member forces. Strength constraints for the auxiliary member forces can be written as

$$-\underline{\sigma} \max_{j=1,2,\ldots,n_S} \{\hat{A}_j\} y_i \le \tilde{N}_i \le \overline{\sigma} \max_{j=1,2,\ldots,n_S} \{\hat{A}_j\} y_i \quad \forall i \in \mathcal{M} \tag{4}$$

4.3. Buckling Constraints
Introducing member buckling constraints to problem P is straightforward. Buckling constraints are written for each member force variable N_{ij}^k as follows

$$N_{ij}^k \ge -\pi^2 \frac{E_i \hat{I}_j}{L_i^2} y_{ij} \quad \forall i \in \mathcal{M},\, j \in \mathcal{P},\, k \in \mathcal{L} \tag{5}$$

where $\hat{I}_j$ is the moment of inertia of the profile alternative j. If profile s is chosen for member i, $y_{is} = 1$, then the force variable N_{is}^k must be greater than $-\pi^2 E_i \hat{I}_s / L_i^2$, which is the buckling strength of profile s of member i. Buckling constraints can be included in the problem by modifying the last constraints as

$$N_{ij}^k \ge \max \left\{ \underline{N}_{ij}^k, -\underline{\sigma}\hat{A}_j, -\pi^2 \frac{E_i \hat{I}_j}{L_i^2} y_{ij} \right\} y_{ij} \quad \forall i \in \mathcal{M},\, j \in \mathcal{P},\, k \in \mathcal{L} \quad \forall i \in \mathcal{M},\, j \in \mathcal{P},\, k \in \mathcal{L} \tag{6}$$

Thus, the problem size is not increased due to buckling constraints.

4.4. Intersecting Members
From the manufacturing point of view, intersecting members may introduce difficulties, in which case they should not be allowed in the solution. In [11], intersecting members are disallowed by a linear constraint in the binary variables y_i. Suppose members y_r and y_s of the ground structure are intersecting. Then, at most one of the two members can be included in the design. This condition is enforced by the constraint

$$y_r + y_s \le 1 \tag{7}$$

This constraint is included for all pairs of intersecting members.

4.5. Member Grouping
Sometimes a group of members should have the same profile. In topology optimization, introducing this condition is not as straightforward as in sizing optimization, since a member belonging to a group may also vanish.

Suppose the members of the group $\mathcal{G} \subseteq \mathcal{M}$ appearing in the truss are to have identical profiles. This condition can be enforced by introducing binary variables $w_j \in \{0,1\}$, $j \in \mathcal{P}$, with the following constraints:

$$\sum_{j=1}^{n_S} w_j \leq 1 \tag{8}$$

$$y_{ij} \leq w_j \quad \forall\, i \in \mathcal{G},\, j \in \mathcal{P} \tag{9}$$

$$\sum_{i \in \mathcal{G}} y_{ij} \geq w_j \quad \forall\, j \in \mathcal{P} \tag{10}$$

The first constraint ensures that at most one profile is selected, but the possibility that the whole group vanishes is allowed. The second constraint implies that if a profile is not chosen ($w_j = 0$), then the corresponding profile variables must be zero. Finally, the third constraint enforces the condition that if a profile is chosen ($w_j = 1$), then one of the profile variables must actually be equal to one. This eliminates the possibility that $w_j = 1$ and $y_{ij} = 0$ for all $i \in \mathcal{G}$.
To the best of the authors' knowledge, the above approach for including member grouping in truss topology optimization has not been presented in the literature before.

5. Distributed Loads

Suppose part of the design domain is subject to a distributed (line) load with magnitude q (Fig. 1a). For simplicity, it is assumed that the load is uniform. Denote the nodes of the ground structure under the line load by $\mathcal{N}_q$. Then, a member is added to the ground structure between each pair of nodes in $\mathcal{N}_q$ (members 4, 5, and 6 in Fig. 1b). Further conditions that prevent the creation of a member between two nodes can be enforced, such as a maximum member length or symmetry of the ground structure. In any case, a number of overlapping members all subject to the line load, are created. Denote the union of the original and the added overlapping members by $\mathcal{M}_q$.

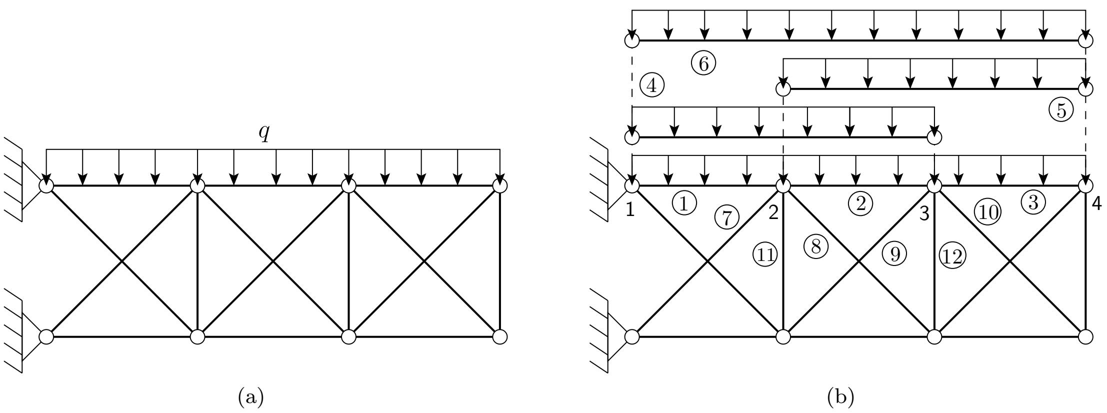

Figure 1: Line loaded truss: (a) original line load; (b) members 4, 5, and 6 are added to the ground structure, and each member 1 to 6 is subject to line load.

Next, for each member $j \in \mathcal{M}_q$, equivalent nodal loads are computed using conventional techniques. For each global degree of freedom, the equivalent nodal loads of the elements connected to the corresponding node are summed. Denote the equivalent nodal load of degree of freedom i due to the distributed load by q_i. It can be written as

$$q_i = \sum_{j \in \mathcal{M}_{\ell(i)}} q_{ij} y_j \tag{11}$$

where $\mathcal{M}_{\ell(i)} \subseteq \mathcal{M}_q$ is the set of members under the line load connected to node ℓ corresponding to the i^{th} degree of freedom, and q_{ij} is the equivalent nodal load of member j related to node ℓ. Note that if member j is removed, $y_j = 0$, then its contribution from q_i is removed.
For example, consider node 2 of Fig. 1b. Members 1, 2, and 5 contribute to the equivalent nodal load. Suppose the length of members 1 and 2 is L and the length of member 5 is $2L$. If the positive direction of the y-axis is up, then the nodal load at node 2 in the y-direction is

$$q_{2y} = -\left(\frac{1}{2}qLy_1 + \frac{1}{2}qLy_2 + \frac{1}{2}q \cdot (2L)y_5\right) \tag{12}$$

The nodal loads q_i due to the line load can be gathered to a load vector

$$\mathbf{q} = \mathbf{Q}\mathbf{y}, \quad \mathbf{Q} \in \mathbb{R}^{n_d \times n_E} \tag{13}$$

and the equilibrium equations become

$$\mathbf{B}\mathbf{N}^k = \mathbf{p}^k + \mathbf{q}^k \quad \Rightarrow \quad \mathbf{B}\mathbf{N}^k - \mathbf{Q}^k\mathbf{y} = \mathbf{p}^k \tag{14}$$

Here, k is the loading condition, where the distributed load is present.
Without further constraints, it is possible that all members subject to the line load vanish. If there are no point loads, i.e. $\mathbf{p}^k = \mathbf{0}$, then the equilibrium equations become $\mathbf{B}\mathbf{N}^k = \mathbf{0}$ with the trivial solution $\mathbf{N}^k = \mathbf{0}$. In order to prevent this, a constraint stating that the sum of the equivalent nodal loads must be equal to the resultant of the line load is added to the problem. Formally, this condition is written as

$$\sum_{i \in \mathcal{U}_x} q_i = F_x - R_x \quad \Rightarrow \quad \sum_{i \in \mathcal{U}_x} \sum_{j \in \mathcal{M}_{\ell(i)}} q_{ij} y_j = F_x - R_x = qL_y - R_x \tag{15}$$

$$\sum_{i \in \mathcal{U}_y} q_i = F_y - R_y \quad \Rightarrow \quad \sum_{i \in \mathcal{U}_y} \sum_{j \in \mathcal{M}_{\ell(i)}} q_{ij} y_j = F_y - R_y = qL_x - R_y \tag{16}$$

where $\mathcal{U}_x$ and $\mathcal{U}_y$ are the global x- and y-directional degrees of freedom, respectively, related to the nodes of the line load, F_x and F_y are the resultants of the distributed load in x and y directions, R_x and R_y are the equivalent loads at supported degrees of freedom, and L_x and L_y are the dimensions of the load in the global x and y directions, respectively.
In the case of the truss in Fig. 1b, the left-hand side of constraint Eq. (16) is

$$\sum_{i \in \mathcal{U}_y} \sum_{j \in \mathcal{M}_{\ell(i)}} q_{ij} y_j = \frac{1}{2}qLy_1 + \frac{1}{2}qLy_2 + \frac{1}{2}q \cdot (2L)y_5 + \frac{1}{2}qLy_2 + \frac{1}{2}qLy_3 + \frac{1}{2}q \cdot (2L)y_4 + \\ + \frac{1}{2}qLy_3 + \frac{1}{2}q(2L)y_5 + \frac{1}{2}q \cdot (3L)y_6 \tag{17}$$

The resultant $qL_x = 3qL$, and the equivalent nodal loads at supported degrees of freedom is

$$R_y = \frac{1}{2}qLy_1 + \frac{1}{2}q(2L)y_4 + \frac{1}{2}q \cdot (3L)y_6 \tag{18}$$

Thus, constraint Eq. (16) becomes (after simplifications)

$$qL(y_1 + y_2 + y_3 + 2y_4 + 2y_5 + 3y_6) = 3qL \tag{19}$$

It remains to write constraints that disallow member overlapping in the optimum structure. Denote by $\mathcal{E}_q(s) \subseteq \mathcal{M}_q$ the set of members partly or fully belonging to the line segment between nodes the consecutive nodes v_s, $v_{s+1} \in \mathcal{N}_q$. Then, for all line segments, the following constraint is written

$$\sum_{i \in \mathcal{E}_q(s)} y_i \leq 1 \tag{20}$$

This constraint means that in a given line segment, only one of the members passing through it can be present in the truss.
For example, the overlapping constraint for the line segment between nodes 1 and 2 in Fig. 1b is

$$y_1 + y_4 + y_6 \leq 1 \tag{21}$$

The constraint of Eq. (20) is not enough to guarantee practical solutions. A further constraint is needed to handle the situation where all ground structure members connected to an interior node (nodes 2 and 3 in Fig. 1b) but not belonging to $\mathcal{M}_q$ vanish. In this case, the node is supported only in the direction of the members in $\mathcal{M}_q$. Such a node is kinematically unstable even though the truss may satisfy the equilibrium equations. The following constraint removes all members of $\mathcal{M}_q$ in this case:

$$y_i \leq \sum_{r \in \overline{\mathcal{M}}_q(s)} y_r \quad \forall\, v_s \in \mathcal{J}_q,\ i \in \mathcal{M}_q(s) \tag{22}$$

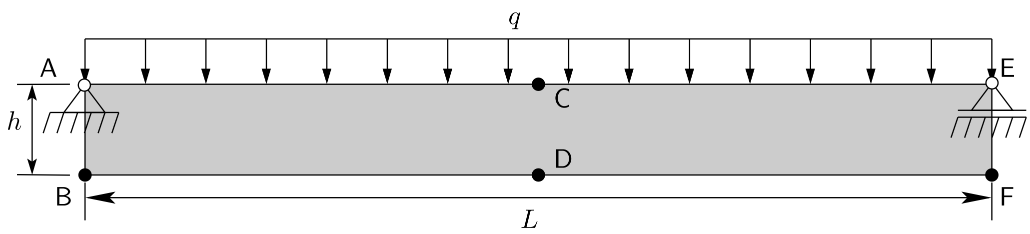

Figure 2: Design domain of the roof truss problem.

where $\mathcal{J}_q \subseteq \mathcal{N}_q$ is the set of interior nodes, $\mathcal{M}_q(s) \subseteq \mathcal{M}_q$ is the set of members connected to node s and $\overline{\mathcal{M}}_q(s)$ is the set of members connected to node s not belonging to $\mathcal{M}_q$.
For node 2, this constraint is

$$y_1 \leq y_7 + y_8 + y_{11} \tag{23}$$
$$y_2 \leq y_7 + y_8 + y_{11} \tag{24}$$
$$y_5 \leq y_7 + y_8 + y_{11} \tag{25}$$

Now if $y_7 = y_8 = y_{11} = 0$, then members 1, 2, 5, must vanish, since they cannot make node 2 kinematically stable. Also, if y_1, then at least one of the members 7, 8, or 11 must be present in order to provide sufficient support for node 2.
Finally, if any ground structure members not belonging $\mathcal{M}_q$ are present and connected to an interior node of $\mathcal{N}_q$, then members of $\mathcal{M}_q$ overlapping that node are not allowed. This condition eliminates situations, where nodes of $\mathcal{N}_q$ are supported by only members not in $\mathcal{M}_q$. This condition is included in the optimization problem by the following constraints:

$$y_i \leq 1 - y_r \quad \forall\, r \in \overline{\mathcal{M}}_q(s),\ s \in \mathcal{J}_q,\ i \in \mathcal{E}_q^o(s) \tag{26}$$

In the above, $\mathcal{E}_q^o(s) \subseteq \mathcal{M}_q$ is the set of members overlapping the node v_s.
For node 2, these constraints are

$$y_4 \leq 1 - y_7 \qquad y_4 \leq 1 - y_8 \qquad y_4 \leq 1 - y_{11} \tag{27}$$
$$y_6 \leq 1 - y_7 \qquad y_6 \leq 1 - y_8 \qquad y_6 \leq 1 - y_{11} \tag{28}$$

Now if any of the members 7, 8, or 11 are present, then members 4 and 6 must vanish. Similarly, if $y_4 = 1$, then members 7, 8, and 11 must vanish.
By appending the minimum weight problem with constraints of Eq. (14), Eq. (15), Eq. (16), Eq. (20), Eq. (22), and Eq. (26), distributed loads can be included in truss topology optimization such that nodes subject to the load are allowed to vanish and the resulting truss still carries all of the load.

6. Example: Roof Truss

6.1. Problem Description

In order to demonstrate the proposed approach for incorporating distributed loads in truss topology optimization, the problem of finding the optimum topology for a roof truss supporting a line loading is considered. The design domain is depicted in Fig. 2. The span of the truss $L = 17000$ mm and the height $h = L/10$. The line load is $q = 41$ kN/m $= 0.041$ kN/mm. The truss is simply supported.
Member profiles are chosen from a set of square hollow sections made of steel, with Young's modulus $E = 210$ GPa, density $\rho = 7850\,\mathrm{kg/m^3}$, and yield strength $f_y = 420$ MPa. The 16 profile alternatives are taken from the catalogue of a Finnish steel manufacturer [3] and the relevant profile data is given in Table 1.
The ground structure is shown in Fig. 3a. The design domain is divided horizontally in 18 intervals of equal length. As a symmetric solution is desired, the ground structure is made symmetric with respect to the line defined by points C and D (Fig. 2) as follows. No diagonal members crossing the line $\overline{CD}$ is allowed and the end points of a horizontal member passing through the line must be equally far from points C and D. A member is created between a pair of nodes, if the distance from one node to the other is at most $L_{\max}$, where $L_{\max} = L/4$. Overlapping members are created at both chords. Constraints of Eq. (20), Eq. (22), and Eq. (26) are included also for the members of the bottom chord. Altogether the ground structure consists of 263 members and 38 nodes with 73 degrees of freedom.

Table 1: Data for profile alternatives. The side length and wall thickness of the section are H and t, respectively.

	H [mm]	t [mm]	A ($10^2\,\mathrm{mm}^2$)	I ($10^4\,\mathrm{mm}^4$)
1	30	3	3.01	3.50
2	40	3	4.21	9.32
3	50	3	5.41	19.47
4	50	4	6.95	23.74
5	60	3	6.61	35.13
6	60	5	10.36	50.49
7	70	3	7.81	57.53
8	70	5	12.36	84.63
9	80	3	9.01	87.84
10	80	5	14.36	131.44
11	90	3	10.21	127.28
12	90	4	13.35	161.92
13	90	6	19.23	220.48
14	100	4	14.95	226.35
15	100	6	21.63	311.47
16	110	4	16.55	305.94

Symmetry of the solution is enforced by variable linking on member existence, profile selection, and nodal variables. To be more specific, if members r and s form a symmetry pair, then $y_r = y_s$ and $y_{rj} = y_{sj}$ for all j, and if nodes ℓ and m form a symmetry pair, then $z_\ell = z_m$.
Finally, members of the chords are grouped such that top chord members form one group and bottom chord members another group. The corresponding binary variables w_j are added to both groups along with the constraints presented in Section 4.5.
All problems are solved by Gurobi 5.0 [7] on a computer with Intel Core i7-3770 processor (8 threads), running at 3.40 GHz clock frequency with 32.0 GB RAM. The problems are solved to global optimality with feasibility tolerance $\epsilon_g = 10^{-7}$ and optimality gap of $\epsilon_f = 10^{-3}$. In other words, at termination, the gap between the best found solution and the lower bound is at most 0.1%.

6.2. Optimum Solutions
First, the minimum weight problem with conventional approach to line loads is solved. In this case the line load is transformed into equivalent nodal loads at the nodes of the top chords. These loads are handled as point forces. Consequently all nodes of the top chord must be present in the solution. This automatically eliminates all overlapping members from the top chord.
The minimum weight design is shown in Fig. 3b. As expected, all nodes of the top chord are present. Several bottom chord nodes have been removed in order to shorten the chord and to make the remaining members longer. As the top chord possesses many nodes, the number of braces is relatively high as well. The minimum weight is $W^* = 687.03\,\mathrm{kg}$. The optimum profiles and utilization ratios are given in Table 2. For each member, the *utilization ratios* for strength and buckling constraints are computed. The utilization ratios are defined by

$$U_{t,N} = \frac{|N|}{f_y A} \tag{29}$$

$$U_{t,B} = \frac{|N|}{\pi^2 \frac{EI}{L^2}} \tag{30}$$

Thus, the closer the utilization ratio is to 1, or 100%, the more efficiently the material of the members is being used. If the utilization ratio is greater than 100%, then the corresponding constraint is violated by the member.
From Table 2, it can be seen that the strength utilization ratio of the chords and some of the braces is over 90%. On the other hand, for many braces, the utilization ratio is below 50%. Possible reasons for this are that either more efficient profiles were not available or that, as all top chord nodes must be present, more braces are required for kinematic stability, and the normal forces of individual braces remain small

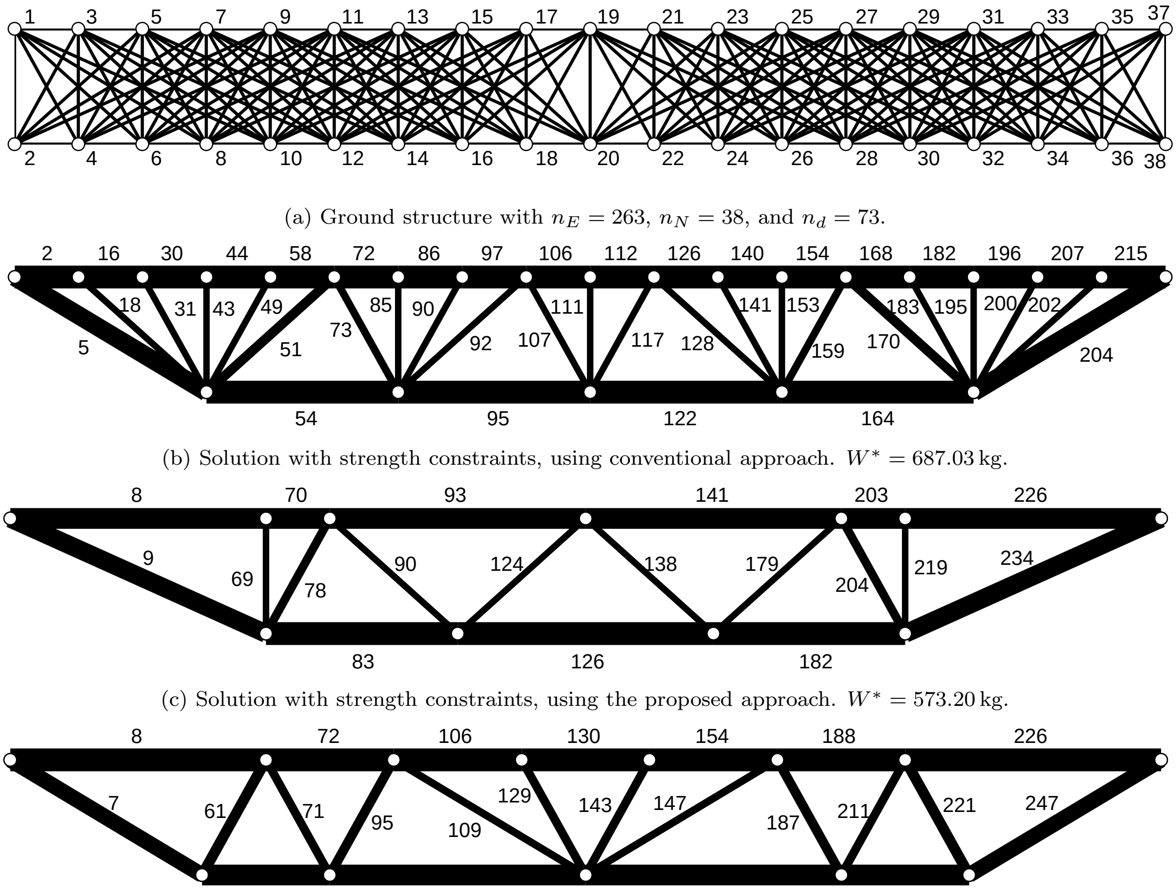

(a) Ground structure with $n_E = 263$, $n_N = 38$, and $n_d = 73$.

(b) Solution with strength constraints, using conventional approach. $W^* = 687.03\,\text{kg}$.

(c) Solution with strength constraints, using the proposed approach. $W^* = 573.20\,\text{kg}$.

(d) Solution with Euler buckling constraints. $W^* = 627.89\,\text{kg}$.

Figure 3: Optimum topologies of the roof truss for different problems. The numbers by the members correspond to the member numbering of the ground structure.

compared with the load carrying capacity of the available profiles. As the buckling length of top chord members is short, Euler buckling constraint is clearly satisfied. However, all braces in compression violate the buckling constraint.

Next, the minimum weight problem is solved with the constraints related to the line load, presented in Section 5, added to the problem. In the first run, member buckling is not considered, and the allowable stress in compression is simply the yield strength, i.e. $\underline{\sigma} = f_y$. The optimum topology is depicted in Fig. 3c. The minimum weight is $W^* = 573.20\,\text{kg}$, which is 16.6% smaller than in the previous case. Thus, the proposed approach for line loads provides a significant improvement to the minimum weight over the conventional approach. Several top chord nodes have been removed, and the remaining nodes are unevenly distributed.

The optimum member profiles and utilization ratios are given in Table 3. In both chords, the strength utilization ratio is over 95%. However, the top chord, which is in compression, does not satisfy the buckling constraints. To be more specific, members, 8, 93, 141, and 226 violate the Euler buckling constraint. In most braces, the strength utilization ratio is over 90%. However, there are members, whose utilization ratios are 76.57% and 87.73%, which suggests that for a broader profile selection, a more efficient solution could have been found.

Finally, Euler buckling constraints, Eq. (5), are included in the problem. The optimum solution is shown in Fig. 3d. The optimum topology differs substantially from the optimum topology without buckling constraints. Braces are located such as to keep the buckling length of the top chord members relatively small but allowing longer members in the bottom chord. The minimum weight is $W^* = 627.89\,\text{kg}$, which is 9.5% higher than the minimum weight of the previous problem, but still 8.6% lower than the first solution.

Table 2: Optimum member profiles and utilization ratios for the problem with conventional approach.

Member	A [mm^2]	$U_{t,N}$ [%]	$U_{t,B}$ [%]
Upper Chord	2163	95.90	12.04
Lower Chord	2163	94.72	–
5, 204	1655	92.03	–
18, 202	301	45.79	515.30
31, 200, 49, 183, 90, 141	301	35.04	230.94
43, 195, 85, 153, 111	301	30.63	154.27
51, 170	661	93.83	231.03
73, 159	421	87.68	–
92, 128	301	68.68	772.95
107, 117	301	17.52	–

Table 3: Minimum weight design and utilization ratios of the solution with strength constraints.

Member	A [mm^2]	$U_{t,N}$ [%]	$U_{t,B}$ [%]
Upper Chord	1923	97.22	245.23
Lower Chord	2163	95.90	–
9, 234	1655	95.03	–
69, 219	301	76.57	385.67
78, 204	541	87.73	186.82
90, 179	301	91.57	–
124, 138	301	91.57	1030.60

Table 4: Minimum weight design and utilization ratios of the solution with Euler buckling constraints.

Member	A [mm^2]	$U_{t,N}$ [%]	$U_{t,B}$ [%]
Upper Chord	2163	99.46	99.87
Lower Chord	1923	95.89	–
7, 247	1335	93.96	–
61, 221	781	94.53	98.35
71, 211	541	77.98	–
95, 187	661	63.82	92.03
109, 147	421	85.13	–
129, 143	541	38.99	83.03

The optimum member profiles and utilization ratios are given in Table 4. The utilization ratio of the upper chord is nearly 100% both for strength and buckling constraints. The utilization ratio of the lower chord is over 95%. For most braces, utilization ratios of over 90% are achieved. As in the previous case, there are also some braces whose utilization ratios are 85% or less.

7. Conclusion

The most important feature of the proposed approach for incorporating distributed loads in truss topology optimization is that it allows ground structure nodes under line load to vanish. As far as the authors are aware, this behaviour cannot be achieved using the conventional techniques for handling distributed loads. Allowing the nodes under line load to vanish is in the spirit of topology optimization, and it provides a broader range of available topologies leading to improved designs.

The problem formulation related to the proposed method requires that the ground structure must be supplemented with overlapping members. Furthermore, binary variables for member and node existence must be included. This might be seen as a drawback especially if the NAND approach is employed in the problem formulation, because of the difficulty of solving mixed integer nonlinear problems with ”black-box” function evaluations. However, with the SAND approach, an explicit MILP formulation is available for truss topology optimization. Including the constraints related to line loads is straightforward for this formulation, and the linearity of the problem is preserved.

Neglecting the bending effects of the line load rises the question of applicability of the formulation in practice. Obviously, it would be appropriate to treat the members under line loads as beams with corresponding constraints for strength and stability. This would change the problem formulation dramatically, as the structure would become a frame with substantially more complicated analysis than the one used for trusses.

8. References

[1] W. Achtziger. Truss topology optimization including bar properties different for tension and compression. *Structural Optimization*, 12, 63–74, 1996.

[2] J.S. Arora and Q. Wang. Review of formulations for structural and mechanical system optimization. *Structural and Multidisciplinary Optimization*, 30, 251–272, 2005.

[3] Rautaruukki Corporation. *Steel sections. Hollow sections*, 2011. Dimensions and cross-sectional properties. `http://www.ruukki.com`.

[4] W. Dorn, R. Gomory, and M. Greenberg. Automatic design of optimal structures. *Journal de Mecanique*, 3, 25–52, 1964.

[5] A.M. Faustino, J.J. Júdice, I.M. Ribeiro, and A.S. Neves. An integer programming model for truss topology optimization. *Investigação Operacional*, 26, 111–127, 2006.

[6] I. E. Grossmann, V. T. Voudouris, and O. Ghattas. Mixed-integer linear programming reformulations for some nonlinear discrete design optimization problems, *Recent advances in global optimization*, C. A. Floudas and P. M. Pardalos (Eds.), pages 478–512. Princeton University Press, 1992.

[7] Gurobi Optimization, Inc. Gurobi optimizer reference manual. `http://www.gurobi.com`, 2012.

[8] Y. Kanno and X. Guo. A mixed integer programming for robust truss topology optimization with stress constraints. *International Journal for Numerical Methods in Engineering*, 83(13), 1675–1699, 2010.

[9] C.D Moen and J.K. Guest. Truss–braced wing topology optimization studies. National institute of aerospace report, NBM Technologies, Inc., Springfield, VA, 2010.

[10] J.M. Oberndorfer, W. Achtziger, and H.R.E.M. Hörnlein. Two approaches for truss topology optimization: a comparison for practical use. *Structural Optimization*, 11, 137–144, 1996.

[11] M. Ohsaki and N. Katoh. Topology optimization of trusses with stress and local constraints on nodal stability and member intersection. *Structural and Multidisciplinary Optimization*, 29, 190–197, 2005.

[12] M.H. Rasmussen and M. Stolpe. Global optimization of discrete truss topology design problems using a parallel cut-and-branch method. *Computers and Structures*, 86, 1527–1538, 2008.